Surface Review and Letters, Vol. 6, No. 6 (1999) 1159–1165

SELF-ENERGY EFFECTS IN THE OPTICAL ANISOTROPY OF GaP(001)

W. G. SCHMIDT,* J. L. FATTEBERT and J. BERNHOLC
Department of Physics, North Carolina State University, Raleigh, NC 27695-8202, USA

F. BECHSTEDT
Institut für Festkörpertheorie und Theoretische Optik,
Friedrich-Schiller-Universität, Max-Wien-Platz 1, 07743 Jena, Germany

Received 12 September 1999

We calculate the reflectance anisotropy for GaP(001)(2×4) surfaces using a real-space multigrid method and *ab initio* pseudopotentials. Our results obtained within DFT-LDA show good qualitative agreement with recent experiments. This holds in particular for the stoichiometric trends. A strong negative anisotropy at low photon energies is linked to the formation of Ga–Ga bonds along the [110] direction. There are discrepancies, however, with respect to the line shape and the energetic positions of characteristic peaks. Substantial improvement is achieved by using a numerically efficient GW approach with approximations for local-field effects and dynamical screening. We find that the spectral features related to transitions between surface perturbed bulk wave functions are more strongly affected by self-energy corrections than anisotropies directly linked to surface electronic states.

1. Introduction

Optical spectroscopy has become an important tool of surface analysis in the last few years due to its high sensitivity and *in situ* applicability.[1] In particular, reflectance anisotropy (difference) spectroscopy (RAS/RDS) is increasingly used to characterize static surfaces and to monitor dynamic surface processes in various environments.[2–4] To fully exploit the technological potential of RAS a theoretical understanding of the underlying physical mechanisms and reliable schemes to calculate RA spectra are needed. The progress in the computational modeling of RAS has been rather slow, however. The agreement between calculated spectra and measured data is often unsatisfactory. This is mainly due to (i) convergence problems caused by the large numerical expense required for calculations of surface optical properties, and (ii) the difficulty in accounting for the many-particle effects in the spectra in an efficient yet accurate manner. Recent attempts to overcome these problems range from a combination of *first-principles* total-energy with tight-binding electronic structure calculations[5,6] to a scissors operator correction of the single-particle energies[7] or a linear parametrization of the quasiparticle shifts with respect to the surface localization of the corresponding electronic states.[8]

In the present work we combine converged *ab initio* calculations within density-functional theory and local-density approximation (DFT-LDA) with a numerically efficient GW approach with approximation for local-field effects and dynamical screening. We study the GaP(001)(2 × 4) surface. That is a suitable model system since experimental data are available for a wide range of surface preparation conditions.[9–11] It is also of technological interest: once the optical response of III–V(001) surfaces is thoroughly understood, their surface status can be determined *in situ*. This will allow control and

*Corresponding author. Permanent address: IFTO, Max-Wien-Platz 1, 07743 Jena, Germany.
E-mail: W.G.Schmidt@ifto.physik.uni-jena.de

optimization of homo- and heteroepitaxial growth processes.

2. Method

Our DFT-LDA calculations are performed using *first-principles* pseudopotentials[12] together with a real-space finite-difference method.[13] A multigrid technique is used for convergence acceleration. The real-space method allows efficient parallelization and is thus particularly suited for the large supercell and many electronic states required for the calculation of the surface dielectric function. The electronic wave functions were mapped on a grid with a spacing of 0.238 Å. To model the surface we used a periodic supercell containing 12 atomic GaP layers, the bottom layer saturated with pseudohydrogen, and a vacuum region equivalent to 8 layers. For the relaxation of the electronic and atomic degrees of freedom we sampled the surface Brillouin zone (SBZ) with four special $\mathbf{k}$ points. The surface dielectric function was calculated including all conduction bands within 8 eV of the top of the valence band and using 16 uniformly distributed $\mathbf{k}$ points in the irreducible part of the SBZ. This corresponds to 256 points in the full (1×1) SBZ. Further details of the DFT-LDA calculation can be found in our earlier study on the optical properties of InP(001).[14]

Calculations within DFT-LDA neglect the quasiparticle character of electrons and typically underestimate excitation energies, an effect known as the band-gap problem.[15] For example, we obtain values of 2.1 and 4.0 eV for the E_0 and E_0' interband transitions of GaP, respectively. The corresponding experimental energies are 2.9 and 4.8 eV.[16] For $E(X_{1c})$ and $E(X_{3c})$ we calculate 1.5 and 1.7 eV. The measured values are 2.1–2.3 and 2.6 eV.[17] Thus the underestimation of the excitation energies close to the fundamental gap amounts to 0.6–0.9 eV.

In order to account for the self-energy effects neglected in DFT-LDA one has to replace the local exchange and correlation potential $V^{\mathrm{XC}}(\mathbf{r})$ by the nonlocal and energy-dependent self-energy operator $\Sigma(\mathbf{r},\mathbf{r}';E)$.[15] However, even in its lowest, the so-called GW approximation, where Σ is expressed as convolution of the single-article propagator G and the dynamically screened Coulomb interaction W, its calculation remains a formidable task. This holds in particular for the large number of states entering the surface dielectric function. Therefore, we introduced further approximations following the schemes developed by Hybertsen and Louie[18] and Bechstedt *et al.*:[19] in first order perturbation theory the GW quasiparticle energies are obtained from the DFT-LDA eigenvalues by

$$E_{n,\mathbf{k}} = E^{\mathrm{LDA}}_{n,\mathbf{k}} + \frac{1}{1+\beta_{n,\mathbf{k}}} \times \left\{ \sum_{n,\mathbf{k}}^{\mathrm{st}} + \sum_{n,\mathbf{k}}^{\mathrm{dyn}} (E^{\mathrm{LDA}}_{n,\mathbf{k}}) - V^{\mathrm{XC}}_{n,\mathbf{k}} \right\}, \quad (1)$$

where the self-energy operator Σ has been divided into static and dynamic contributions. $\beta_{n,\mathbf{k}}$ is the linear term of the expansion of Σ^{dyn} in energy around the DFT-LDA eigenvalue $E^{\mathrm{LDA}}_{n,\mathbf{k}}$. The static part can be further divided into two parts:

$$\begin{aligned}\Sigma^{\mathrm{st}}(\mathbf{r},\mathbf{r}') &= \frac{1}{2}\sum_{n,\mathbf{k}} \psi_{n,\mathbf{k}}(\mathbf{r})\psi^*_{n,\mathbf{k}}(\mathbf{r}')\{W(\mathbf{r},\mathbf{r}';0) - v(\mathbf{r}-\mathbf{r}')\} \\ &\quad - \sum_{v,\mathbf{k}} \psi_{v,\mathbf{k}}(\mathbf{r})\psi^*_{v,\mathbf{k}}(\mathbf{r}')W(\mathbf{r},\mathbf{r}';0)\,, \end{aligned} \quad (2)$$

representing the Coulomb hole Σ_{COH} and the screened exchange Σ_{SEX}. The $\psi_{n,\mathbf{k}}$ are the DFT-LDA wave functions and $W(\mathbf{r},\mathbf{r}';0)$ and $v(\mathbf{r}-\mathbf{r}')$ denote the statically screened and bare Coulomb potentials, respectively. For the practical calculation of W we model the dielectric function as[19]

$$\epsilon(q) = 1 + \{(\epsilon_\infty - 1)^{-1} + (q/q_{\mathrm{TF}})^2 + 3q^4/(4k_{\mathrm{F}}^2 q_{\mathrm{TF}}^2)\}^{-1}\,, \quad (3)$$

where k_{F} and q_{TF} represent the Fermi and Thomas–Fermi wave vectors, respectively. This expression interpolates between the correct behaviors at high and low q vectors and yields by construction the static dielectric constant for $q = 0$. This model reproduces very well the RPA results for semiconductors.[20] Using the local-density approximation for W of Ref. 18, Σ_{COH} can now be calculated analytically,[19] resulting in a potential that depends on the local charge density via k_{F} and q_{TF}. For the calculation of Σ_{SEX} we retain only diagonal elements in the Fourier transform of W. The local fields are included, however, by using state-dependent charge densities

$$\rho_{n,\mathbf{k}} = \int d\mathbf{r}^3 \rho(\mathbf{r}) |\psi_{n,\mathbf{k}}(\mathbf{r})|^2\,, \quad (4)$$

in the calculation of k_{F} and q_{TF}. The dynamic terms $\beta_{n,\mathbf{k}}$ and Σ^{dyn} in (1) can be approximated by simple integrals of the dielectric function.[19] For the practical calculation we use (3) together with a single plasmon pole approximation to describe the frequency dependence. Local-field effects are again included using the mean-density approximation (4) in the dielectric function.

Applying this approach to the DFT-LDA bulk band structure of GaP we obtain interband transition energies of 2.7 and 4.8 eV for E_0 and E_0', respectively. $E(X_{1c})$ and $E(X_{3c})$ are shifted to 2.2 and 2.4 eV. These values agree with experiment within 0.2 eV. The application of the GW scheme to the surface seems problematic, since the model requires the input of the dielectric constant ϵ_∞. Northrup[21] and Rohlfing *et al.*[22] have shown, however, that the inaccuracies caused by the use of bulk dielectric constants for surface GW calculations are very small.

Finally, the slab polarizability was calculated in the independent-particle approximation based on the electronic structure obtained either within DFT-LDA or GWA. In the latter case, we corrected the transition matrix elements according to Ref. 23. We determine the reflectance anisotropy form the polarizability using the formalism developed by the Del Sole[24] and Manghi *et al.*[25]

3. Results

Total-energy calculations[10,26,27] for GaP(001) predict a sequence of (2×4) single-dimer reconstructions for cation-rich surfaces. $\beta2(2\times4)$ and $c(4\times4)$ reconstructions, known from GaAs(001), form for more P-rich surfaces. A top view of the GaP surface models is given in Fig. 1. These theoretical findings agree with the recent experiments, as discussed in detail in Refs. 10 and 27.

In Fig. 2 we show the RA spectra calculated within DFT-LDA for the four (2×4) surface structures shown in Fig. 1. The top-Ga-dimer, mixed-dimer and δ structures show a pronounced negative anisotropy in the low energy region, with minima between 2.0 and 2.3 eV. The strength of that anisotropy is directly correlated with the number of Ga–Ga bonds along the [110] direction. Its magnitude is highest for the top-Ga-dimer model with eight bonds, slightly reduced and shifted to lower energies for the mixed-dimer geometry with six cation–cation bonds, and flattened for the δ structure with only two such bonds. The calculated spectra also show a strong dependence on the structural details at higher energies. For the $\beta2$ geometry with three P–P dimers oriented along $[1\bar{1}0]$ we find a relatively broad positive anisotropy between about 2.4 and 4.4 eV. Maxima of the anisotropy appear around 3.2 and 4.1 eV and a shoulder exists at 2.8 eV. The shape of that anisotropy is roughly preserved for the δ structure, which features one P–P dimer. The magnitude of this anisotropy is, however, somewhat reduced and the spectrum is shifted downwards. An even further reduction in positive anisotropy occurs for the mixed-dimer and top-Ga-dimer structures, featuring single Ga–P or Ga–Ga dimers, respectively, on top of a Ga-terminated substrate. The evolution of the spectra in the high energy region shows thus a correlation between the positive anisotropy and the formation of P–P dimers. We mention that a very similar trend

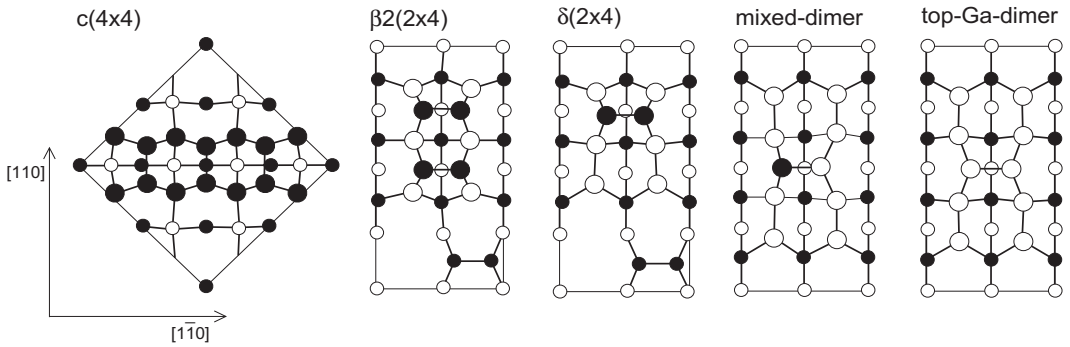

Fig. 1. Top view of GaP(001)(2×4) surface reconstruction models. The structures are ordered according to their stoichiometry. Empty (filled) circles represent Ga(P) atoms. Large (small) symbols indicate positions in the first and second (third and fourth) atomic layers.

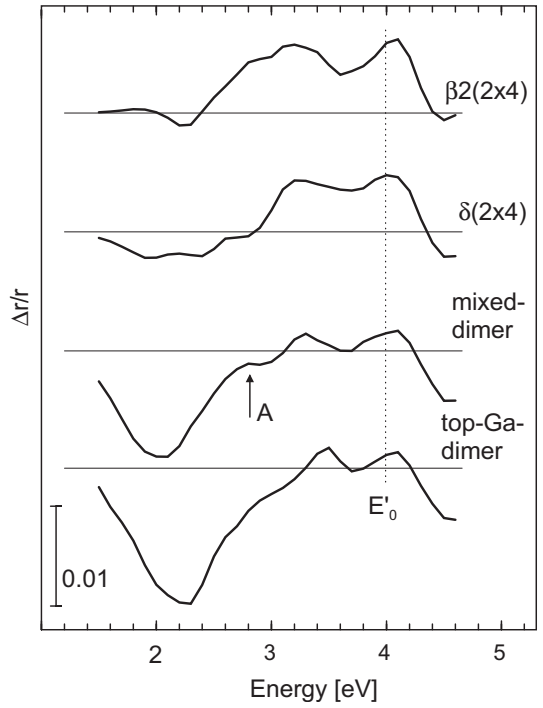

Fig. 2. RA spectra $[\mathrm{Re}\{(r_{[\bar{1}10]} - r_{[110]})/\langle r\rangle\}]$ calculated within DFT-LDA for the four GaP(001)(2 × 4) surface reconstruction models shown in Fig. 1. The calculated position of E_0' is indicated.

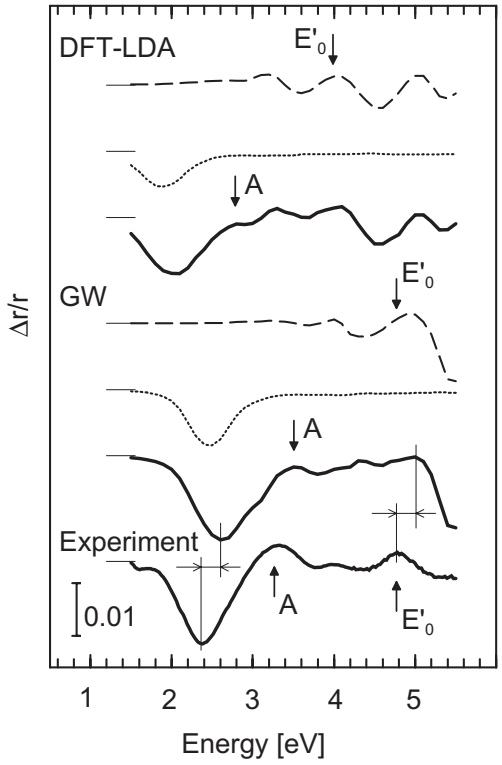

Fig. 3. RA spectra $[\mathrm{Re}\{(r_{[\bar{1}10]} - r_{[110]})/\langle r\rangle\}]$ calculated within DFT-LDA/GWA for the mixed-dimer structure are compared with the measured data[10] for the Ga-rich GaP(001)(2 × 4) surface. The calculated/measured positions of E_0' are indicated. Dashed and dotted lines show the contributions to the RA from transitions between subsurface electronic states and from transitions between the surface states $V1$–$V3$ and $C1$–$C5$, respectively (cf. Fig. 4). Solid lines represent the calculations for the complete slab.

was found in experimental[28] and theoretical studies on InP(001).[14]

Our calculations are in accord with the available experimental data.[9–11] The RA spectra measured for the Ga-rich phase of GaP(001)(2 × 4) feature a strong negative peak around 2.4 eV. That peak disappears as the surface gets more P-rich. Both the top-Ga-dimer model and the mixed-dimer model thus appear plausible candidates to explain the Ga-rich surface phase. The measured spectrum for the Ga-rich phase shows a maximum between the energies of the E_0 and E_1 critical points (CPs). This peak, which should be observed between 2.1 and 2.9 eV in the calculated spectrum, is absent in case of the top-Ga-dimer structure; it appears, however, as a weak shoulder (denoted A in Fig. 2) for the mixed-dimer model. As will be discussed below, the agreement between the calculated spectrum for the mixed-dimer structure and the measured RA improves substantially upon inclusion of self-energy effects, in particular with respect to the shoulder A. On the basis of the calculated RA we thus tentatively identify the Ga-rich phase of GaP(001)(2 × 4) with the mixed-dimer model. This assignment is corroborated by the recently measured surface core-level shifts:[29] two surface Ga components were assigned to threefold-coordinated Ga atoms and Ga–Ga bonds. These two components can be explained both by the top-Ga-dimer structure and the mixed-dimer model. Only the latter, however, explains the measured surface P component, supposed to arise from threefold-coordinated P atoms. This indicates that the extreme Ga-rich limit, which according to the total-energy calculations[10,27] is characterized by the top-Ga-dimer model, may actually not be reached experimentally.

The measured spectrum for the less Ga-rich (2 × 4) surface phase[10] is dominated by a "camelback" overall spectrum shape with maxima between the energies of the E_0 and E_1 CPs and at E_0'. No negative

anisotropy appears. The only computed spectrum with no (or very little) negative anisotropy belongs to the $\beta 2(2\times4)$ structure. Maxima appear at 3.2 and 4.1 eV, close to the calculated energies of the E_1 and E_0' CPs. Our results thus indicate that the P-rich phase of the GaP(001)(2×4) surface corresponds to the $\beta 2(2 \times 4)$ structure in analogy to As-rich GaAs(001) surfaces.

In the following we focus on the Ga-rich surface phase, which corresponds to the mixed-dimer structure as discussed above. This structure is reproducibly obtained in experiments.[10,11,29] It is also interesting from a theoretical point of view, as it shows both bulk- and surface-related features in its optical spectrum, as will be discussed below.

To determine the origin of the optical anisotropy, we spatially separated the contributions to the RA from different slab regions. The dashed curves in Fig. 3 show the anisotropy due to transitions between the electronic states localized below the top four atomic layers. It is obvious that the surface modification of these wave functions gives rise to strong anisotropies for high photon energies. In particular, a feature occurs near the calculated energy of the E_0' CP of the GaP bulk band structure. This bulk-related feature depends only weakly on the actual surface structure: it is present in the calculated spectra of all structures included in our study (cf. Fig. 2). Experimentally, the maximum at the E_0' CP was found irrespective of the surface preparation conditions.[10,11]

On the other hand, strong anisotropies in the low-energy part of the spectrum arise from transitions between surface localized states. In Fig. 4 we show the surface bands of the mixed-dimer model calculated in DFT-LDA, together with their orbital character. The highest occupied surface state, $V1$, slightly above the bulk valence band maximum (VBM), corresponds to the P dangling bond at the mixed dimer. $V2$ and $V3$, slightly below the VBM, are related to σ bonds between surface Ga atoms. $C1$–$C5$, in the upper part of the bulk band gap, arise from dangling bonds at the second-layer surface cations. [For a detailed discussion of the GaP(001) surface electronic structure, see Ref. 27.] In particular, transitions between Ga–Ga bond-related states and empty Ga dangling bonds cause a strong negative anisotropy around 2 eV. The dotted lines in Fig. 3 show the RA induced exclusively by transitions between the valence states $V1$, $V2$ and $V3$ and the conduction states $C1$–$C5$. These eight states nearly completely account for the negative anisotropy observed at low

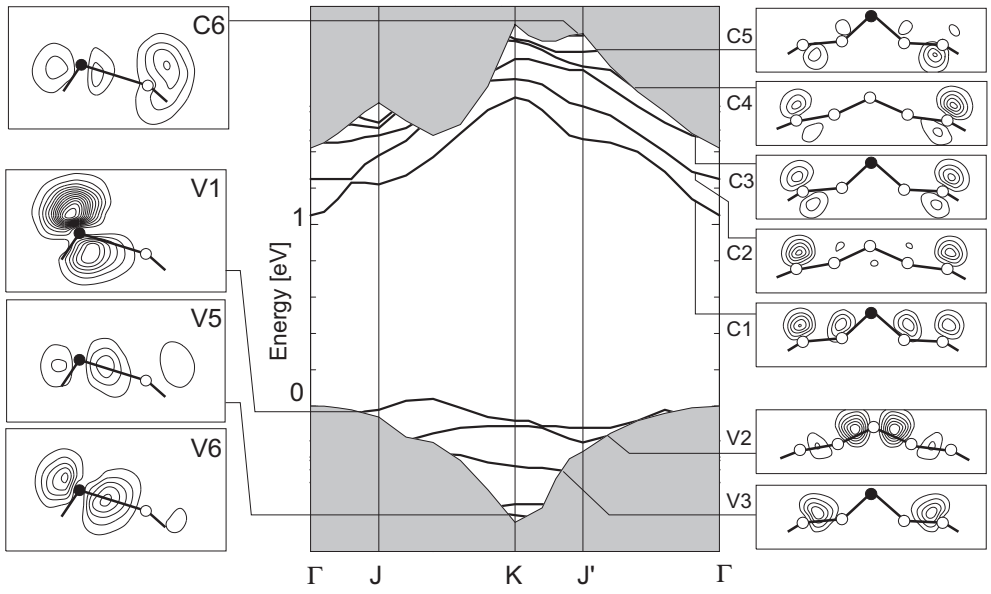

Fig. 4. Surface band structure (bound states) for the mixed-dimer structure of GaP(001). Gray regions indicate the projected bulk band structure. In the left and right panels the corresponding squared wave functions at K are shown. The contour spacing is 10^{-3} bohr^{-3}.

photon energies. The assignment of cation-related surface states to the RA around 2 eV corroborates the phenomenological link established by comparing the RA of different structures as discussed above.

The optical anisotropy calculated for the complete slab (solid lines in Fig. 3) corresponds roughly to a superposition of the bulk-related features and surface peaks discussed above. This is a theoretical confirmation of Aspnes and Studna, who discriminated in their pioneering work on reflectance anisotropy[30] between two components: "intrinsic" contributions from surface effects on bulk wave functions and "extrinsic" contributions related to the surface structure.

In Fig. 3 two sets of theoretical data are presented, obtained in DFT-LDA and GWA. As expected from the shifts calculated for the GaP bulk band structure, we observe a distinct blueshift of the spectrum upon inclusion of self-energy effects. However, the shift is nonuniform: it amounts to about 0.6 eV for the surface-state related features (dotted lines) and 0.8–1.0 eV for the bulk-related ones (dashed lines). This agrees with a study by Hybertsen and Louie,[31] who found that, depending on their orbital character, surface states may actually be less affected by self-energy effects than bulk states. The nonuniformity of the calculated quasiparticle shifts agrees with experiment: as indicated by the arrows in the lower part of Fig. 3, the energy shift between the measured data and the spectrum calculated in GWA is nearly constant and amounts to about 0.3 eV. The inclusion of self-energy effects in the calculations does not only lead to energy shifts, but also to pronounced changes in the line shape. The weak shoulder A at 2.8 eV in the DFT-LDA spectrum develops into a maximum at 3.5 eV, in good agreement with experiment.

While the agreement between the measured and the calculated spectra improves much upon inclusion of GW corrections, there remain discrepancies: the excitation energies are somewhat overestimated and the line shapes, in particular for higher energies, do not agree very well. That is not too astonishing: one limitation of our study is the neglect of electron–hole interactions.[32] Furthermore, the LDA-like treatment of local-field effects in our GWA model only approximates the screening across the highly inhomogenous surface region. Finally, our calculations are performed for an ideal surface, neglecting defects and domain boundaries. Such imperfections are expected to induce distinct features in the optical anisotropy.[33]

4. Summary

We carried out an extensive theoretical study on the optical anisotropy of GaP(001)(2×4) surfaces. The calculated RA spectra show characteristic "signatures" from surface states. In particular, the transitions between Ga–Ga bonding states and empty Ga dangling bonds give rise to a strong negative anisotropy at low photon energies. The strength of this anisotropy is directly related to the number of cation–cation bonds at the surface. In addition, we find derivative-like features caused by surface-modified bulk wave functions. These features depend only little on the actual surface structure. The results obtained within DFT-LDA give a reasonable qualitative description of the experimental spectra. We also investigated the influence of self-energy effects on the calculated reflectance anisotropy, using a numerically efficient GW scheme with approximations for local-field effects and the dynamical screening. The inclusion of self-energy effects leads to a much improved agreement with experiment, both with respect to characteristic peak positions and the calculated line shape.

Acknowledgments

We acknowledge support by DFG (Schm 1361/1-1), NSF (DMR 9408437) and ONR (N00014-96-I-0161), as well as grants of computer time from the DoD Challenge Program and the North Carolina Supercomputing Center.

References

1. *Epioptics. Linear and Nonlinear Optical Spectroscopy of Surfaces and Interfaces*, eds. J. F. McGilp, D. Weaire and C. H. Patterson (Springer-Verlag, Berlin, 1995).
2. W. Richter, *Philos. T. Roy. Soc.* **A344**, 453 (1993).
3. D. E. Aspnes, *Surf. Sci.* **309**, 1017 (1994).
4. Z. Sobiesierski, D. I. Westwood and C. C. Matthai, *J. Phys.: Cond. Matter* **10**, 1 (1998).
5. P. V. Santos, B. Koopmans, N. Esser, W. G. Schmidt and F. Bechstedt, *Phys. Rev. Lett.* **77**, 759 (1996).
6. A. I. Shrebtii, N. Esser, W. Richter, W. G. Schmidt, F. Bechstedt, B. O. Fimland, A. Kley and R. Del Sole, *Phys. Rev. Lett.* **81**, 721 (1998).

7. L. Kipp, D. K. Biegelsen, J. E. Northrup, L.-E. Swartz and R. D. Bringans, *Phys. Rev. Lett.* **76**, 2810 (1996).
8. O. Pulci, G. Onida, R. Del Sole and L. Reining, *Phys. Rev. Lett.* **81**, 5374 (1998).
9. P. A. Postigo, G. Armelles, T. Utzmeier and F. Briones, *Phys. Rev.* **B57**, 1359 (1998).
10. A. M. Frisch, W. G. Schmidt, J. Bernholc, M. Pristovsek, N. Esser and W. Richter, *Phys. Rev.* **B60**, 2488 (1999).
11. M. Zorn, B. Junno, T. Trepk, S. Bose, L. Samuelson, J.-T. Zettler and W. Richter, *Phys. Rev. B* (submitted).
12. M. Fuchs and M. Scheffler, *Comput. Phys. Commun.* **119**, 67 (1999).
13. E. L. Briggs, D. J. Sullivan and J. Bernholc, *Phys. Rev.* **B54**, 14362 (1996).
14. W. G. Schmidt, E. L. Briggs, J. Bernholc and F. Bechstedt, *Phys. Rev.* **B59**, 2234 (1999).
15. F. Aryasetiawan and O. Gunnarsson, *Rep. Prog. Phys.* **61**, 237 (1998).
16. S. Zollner, M. Garriga, J. Kirchner, J. Humlíček, M. Cardona and G. Neuhold, *Phys. Rev.* **B48**, 7915 (1993).
17. *Landolt-Börnstein, Numerical Data and Functional Relationships in Science and Technology* (Springer-Verlag, Berlin, 1982), Vol. III, 17a.
18. M. S. Hybertsen and S. G. Louie, *Phys. Rev.* **B37**, 2733 (1988).
19. F. Bechstedt, R. Del Sole, G. Cappellini and L. Reining, *Solid State Commun.* **84**, 765 (1992).
20. G. Cappellini, R. Del Sole, L. Reining and F. Bechstedt, *Phys. Rev.* **B47**, 9892 (1993).
21. J. E. Northrup, *Phys. Rev.* **B47**, 10032 (1993).
22. M. Rohlfing, P. Krüger and J. Pollmann, *Phys. Rev.* **B52**, 1905 (1995).
23. R. Del Sole and R. Girlanda, *Phys. Rev.* **B48**, 11789 (1993).
24. R. Del Sole, *Solid State Commun.* **37**, 537 (1981).
25. F. Manghi, R. Del Sole, A. Selloni and E. Molinari, *Phys. Rev.* **B41**, 9935 (1990).
26. S. Mirbt, N. Moll, K. Cho and J. D. Joannopoulos, *Phys. Rev. B* (submitted).
27. W. G. Schmidt, J. Bernholc and F. Bechstedt, *Appl. Surf. Sci.* (submitted).
28. K. B. Ozanyan, P. J. Parbrook, M. Hopkinson, C. R. Whitehouse, Z. Sobiesierski and D. I. Westwood, *J. Appl. Phys.* **82**, 474 (1997).
29. N. Sanada, S. Mochizuki, S. Ichikawa, N. Utsumi, M. Shimomura, G. Kaneda, A. Takeuchi, Y. Suzuki, Y. Fukuda, S. Tanaka and M. Kamata, *Surf. Sci.* **419**, 120 (1999).
30. D. E. Aspnes and A. A. Studna, *Phys. Rev. Lett.* **54**, 1956 (1985).
31. M. S. Hybertsen and S. G. Louie, *Phys. Rev.* **B38**, 4033 (1988).
32. S. Albrecht, L. Reining, R. Del Sole and G. Onida, *Phys. Rev. Lett.* **80**, 4510 (1998).
33. S. G. Jaloviar, J.-L. Lin, F. Liu, V. Zielasek, L. McCaughan and M. G. Lagally, *Phys. Rev. Lett.* **82**, 791 (1999).